A SIMPLIFIED IMPEDANCE MODEL FOR ADHESIVELY-BONDED PIEZO-IMPEDANCE TRANSDUCERS

Suresh Bhalla[1] , Praveen Kumar[2], Ashok Gupta[3] and Tushar K. Datta[4]

ABSTRACT

The electro-mechanical impedance (EMI) technique employs surface-bonded lead zirconate titanate piezo-electric ceramic (PZT) patches as impedance transducers for structural health monitoring (SHM) and non-destructive evaluation (NDE). The patches are bonded to the monitored structures using finitely thick adhesive bond layer, which introduces shear lag effect, thus invariably influencing the electro-mechanical admittance signatures. This paper presents a new simplified impedance model to incorporate shear lag effect into electro-mechanical admittance formulations, both 1D and 2D. This provides a closed-form analytical solution of the inverse problem, i.e to derive the true structural impedance from the measured conductance and susceptance signatures, thus an improvement over the existing models. The influence of various parameters (associated with the bond layer) on admittance signatures is investigated using the proposed model and the results compared with existing models. The results show that the new

[1] (Corresponding author) Assistant Professor, Civil Engineering Department, Indian Institute of Technology Delhi, New Delhi, India 110 016, Email: sbhalla@civil.iitd.ac.in, Tel: (91-11) 2659-1040 Fax: (91-11) 2658-1117

[2] Engineer, Central Public Works Department, New Delhi 110001 (formerly M. Tech. student, Civil Engineering Department, Indian Institute of Technology Delhi), Email: praveenk96@gmail.com

[3] Professor, Department of Civil Engineering, Indian Institute of Technology Delhi, New Delhi, India 110016, Email: ashokg@civil.iitd.ac.in

[4] Dogra Chair Professor, Department of Civil Engineering, Indian Institute of Technology Delhi, New Delhi, India 110016, Email: tkdatta@civil.iitd.ac.in

model, which is far simpler than the existing models, models the shear lag phenomenon reasonably well besides providing direct solution of a complex inverse problem.

CE Database Headings: Elastic Analysis; Sensors; Shear Lag; Piezoelectricity

Key Words: Electro-mechanical impedance (EMI) technique; adhesive; shear lag; structural health monitoring (SHM); conductance; susceptance.

INTRODUCTION

This paper is primarily focused on development of a simplified analytical model for shear lag effect inherent in adhesively bonded PZT patches for direct use in SHM/ NDE through the EMI technique. The EMI technique, which originated over one and a half decade ago, is now very widely accepted as a cost effective and highly sensitive technique for SHM and NDE of a variety of engineering systems (Sun et al. 1995; Soh et al. 2000; Park et al. 2000; Giurgiuiu and Zagrai 2002; Bhalla and Soh 2003; Park et al. 2006). This technique makes use of the PZT patches as impedance transducers (Bhalla and Soh 2004a, b) by utilizing their direct and converse piezoelectric properties simultaneously. The structural component to be monitored is instrumented with a PZT patch on the surface, which is excited through an alternating voltage signal using an impedance analyzer/ LCR meter, sweeping through a particular frequency range (of the order of tens to hundreds of kHz). At any particular frequency, the patch actuates the structure and the structural response is simultaneously sensed and measured by the patch in terms of electromechanical admittance, consisting of conductance (the real component), and susceptance (the imaginary component). In this manner, frequency plots, termed conductance and susceptance signatures, are generated. Any change in the condition of the structure manifests itself as a deviation in these signatures, which is utilized for SHM and NDE, considering the signatures of the healthy state structure as the baseline. Owing to the high frequency of excitations (30 - 400 kHz range), the damage sensitivity of the EMI technique is far higher than any of the conventional NDE techniques, say global vibration techniques or local NDE techniques (Park et al. 2000).

The PZT patches, which play the key role in the EMI technique, typically develop surface charges under mechanical stresses and conversely undergo mechanical deformations when subjected to electric fields, as expressed mathematically by (IEEE standard 1987)

$$D_i = \overline{\varepsilon_{ij}^T} E_j + d_{im} T_m \tag{1}$$

$$S_k = d_{jk} E_j + \overline{s_{km}^E} T_m \tag{2}$$

where D_i is the electric displacement, S_k the mechanical strain, E_j the electric field and T_m the mechanical stress. $\overline{\varepsilon_{ij}^T}$ denotes the complex electric permittivity of the PZT material at constant stress, d_{im} and d_{jk} the piezoelectric strain coefficients (or constants) and $\overline{s_{km}^E}$ the complex elastic compliance at constant electric field. The superscripts '*T*' and '*E*' indicate that the quantity has been measured at constant stress and constant electric field respectively.

During the last one and half decades, several attempts have been made to model the PZT-structure electromechanical interaction. The beginning was made by Crawley and de Luis (1987) in the form of 'static approach', later substituted by the 'impedance approach' of Liang, et al. (1994). Liang and coworkers modelled the host structure as mechanical impedance Z_s connected to the PZT patch at the end, as shown in Fig. 1(a), with the patch undergoing axial vibrations under an alternating electric field E_3. Mathematically, Z_s is related to the force F and the velocity $\dot{u}$ by

$$F_{(x=l)} = -Z_S \dot{u}_{(x=l)} \tag{3}$$

Solution of the governing 1D wave equation resulted in following expression for the complex electromechanical admittance for the system of Fig. 1(a)

$$\overline{Y} = G + Bj = \omega j \frac{wl}{h}\left[(\overline{\varepsilon_{33}^{T}} - d_{31}^{2}\overline{Y^{E}}) + \left(\frac{Z_a}{Z_S + Z_a}\right) d_{31}^{2}\overline{Y^{E}}\left(\frac{\tan \kappa l}{\kappa l}\right)\right] \tag{4}$$

where w, l and h represent the PZT patch's dimensions (see Fig. 1a), d_{31} the piezoelectric strain coefficient for the 1-3 axes and ω the angular frequency. $\overline{Y^{E}} = Y^{E}(1+\eta j)$ is the complex Young's modulus of the PZT patch (at constant electric field) and $\overline{\varepsilon_{33}^{E}} = \varepsilon_{33}^{E}(1-\delta j)$ the complex electric permittivity (at constant stress), with the symbols η and δ denoting the mechanical loss factor and the dielectric loss factor respectively. Z_a represents the mechanical impedance of the PZT patch (in short circuited condition), given by

$$Z_a = \frac{\kappa w h}{\tan \kappa l}\frac{\overline{Y^{E}}}{(j\omega)} \tag{5}$$

where κ, the wave number, is related to the density ρ and the Young's modulus $\overline{Y^{E}}$ of the patch by

$$\kappa = \omega\sqrt{\frac{\rho}{\overline{Y^{E}}}} \tag{6}$$

In real-life applications, where the PZT patch is surface-bonded on a structure, the nodal plane passes through the centre line of the patch, as shown in Fig. 1(b). The structure can be represented as a set of impedances Z_s connected on the either side of the patch, as illustrated in Fig. 1(c). For this scenario, l would be the half-length of the patch and Eq. (4) needs to be modified as

$$\overline{Y} = G + Bj = 2\omega j \frac{wl}{h}\left[(\overline{\varepsilon_{33}^{T}} - d_{31}^{2}\overline{Y^{E}}) + \left(\frac{Z_a}{Z_S + Z_a}\right) d_{31}^{2}\overline{Y^{E}}\left(\frac{\tan \kappa l}{\kappa l}\right)\right] \tag{7}$$

Zhou et al. (1996) extended the formulations of Liang to model the a PZT element coupled to a 2D host structure. The related physical model is schematically illustrated in Fig. 2. Zhou and

coworkers replaced the single term Z_s by a matrix consisting of the direct impedances Z_{xx} and Z_{yy}, and the cross impedances Z_{xy} and Z_{yx}, related to the planar forces F_1 and F_2 (along axes 1 and 2 respectively) and the corresponding planar velocities $\dot{u}_1$ and $\dot{u}_2$ by

$$\begin{bmatrix} F_1 \\ F_2 \end{bmatrix} = -\begin{bmatrix} Z_{xx} & Z_{xy} \\ Z_{yx} & Z_{yy} \end{bmatrix} \begin{bmatrix} \dot{u}_1 \\ \dot{u}_2 \end{bmatrix} \tag{8}$$

Considering dynamic equilibrium along the two principal axes in conjunction with piezoelectric constitutive relations (Eqs. 1 and 2), they derived

$$\overline{Y} = j\omega \frac{wl}{h} \left[\overline{\varepsilon_{33}^T} - \frac{2d_{31}^2 \overline{Y^E}}{(1-\nu)} + \frac{d_{31}^2 \overline{Y^E}}{(1-\nu)} \left\{ \frac{\sin \kappa l}{l} \quad \frac{\sin \kappa w}{w} \right\} \begin{Bmatrix} \kappa \cos(\kappa l) \left\{ 1 - \nu \frac{w}{l} \frac{Z_{xy}}{Z_{axx}} + \frac{Z_{xx}}{Z_{axx}} \right\} & \kappa \cos(\kappa w) \left\{ \frac{l}{w} \frac{Z_{yx}}{Z_{ayy}} - \nu \frac{Z_{yy}}{Z_{ayy}} \right\} \\ \kappa \cos(\kappa l) \left\{ \frac{w}{l} \frac{Z_{xy}}{Z_{axx}} - \nu \frac{Z_{xx}}{Z_{axx}} \right\} & \kappa \cos(\kappa w) \left\{ 1 - \nu \frac{l}{w} \frac{Z_{yx}}{Z_{ayy}} + \frac{Z_{yy}}{Z_{ayy}} \right\} \end{Bmatrix}^{-1} \begin{Bmatrix} 1 \\ 1 \end{Bmatrix} \right] \tag{9}$$

where κ, the 2D wave number, is given by

$$\kappa = \omega \sqrt{\frac{\rho(1-\nu^2)}{\overline{Y^E}}} \tag{10}$$

Z_{axx} and Z_{ayy} are the two components of the mechanical impedance of the PZT patch along the two principal directions, given by Eq. 5. Although the analytical derivations of Zhou and co-workers are accurate in themselves, the experimental difficulties prohibit their direct application for the inverse problem, i.e. the extraction of host structure's mechanical impedance. Using the EMI technique, one can experimentally obtain two quantities- G and B for a surface-bonded PZT patch. If complete information about the structure is desired, Eq. (9) needs to be solved for 4 complex unknowns- Z_{xx}, Z_{yy}, Z_{xy}, Z_{yx} (or 8 real unknowns). Hence, the model could not be employed for the experimental determination of the drive point mechanical impedance from measurements alone.

To alleviate these shortcomings, the concept of 'effective impedance' was introduced by Bhalla and Soh (2004a). The related physical model is shown in Fig. 3 for a square-shaped PZT patch of half-length *l*. bhalla and Soh (2004a) represented the PZT-structure interaction in the form of boundary traction *f* per unit length, varying harmonically with time. The 'effecive mechanical impedance', $Z_{a,eff}$, of the patch was defined as

$$Z_{a,eff} = \frac{F_{eff}}{\dot{u}_{eff}} = \frac{\oint_S \vec{f}.\hat{n}\,ds}{\dot{u}_{eff}} = \frac{2h\overline{Y^E}}{j\omega(1-\nu)\overline{T}} \tag{11}$$

where F_{eff} is the overall planar force (or the effective force) causing area deformation of the PZT patch and $\hat{n}$ is the unit vector normal to the boundary. $u_{\text{eff}} = \delta A/p_o$ is the 'effective displacement', with δA denoting the change in the patch's area and p_o its original undeformed perimeter. Differentiation of the effective displacement with respect to time yields the effective velocity, $\dot{u}_{eff}$. The effective drive point impedance of the host structure can be similarly defined, by applying a force on the surface of the host structure, along the boundary of the proposed location of the PZT patch. The term $\overline{T}$ is the complex tangent ratio, theoretically equal to [tan(κl) /κl]. However, in actual situations, it needs correction to realistically consider the deviation of the PZT patch from the ideal behavior, to accommodate which Bhalla and Soh (2004a) introduced correction factors as

$$\overline{T} = \begin{cases} \dfrac{\tan(C\kappa l)}{C\kappa l} & \text{for single-peak behavior.} \\ \dfrac{1}{2}\left(\dfrac{\tan C_1\kappa l}{C_1\kappa l} + \dfrac{\tan C_2\kappa l}{C_2\kappa l}\right) & \text{for twin-peak behavior.} \end{cases} \tag{12}$$

The correction factors C_1 and C_2 (or C), and whether the patch conforms to 'single-peak' or 'twin-peak' behaviour, can be determined from the experimentally obtained conductance and susceptance signatures of the PZT patch in 'free-free' conditions before bonding it on the host structure, as outlined by Bhalla and Soh (2004a). It has been demonstrated by that this 'updating' enables a much more accurate reults. Solution of the governing 2D wave equation for this system yielded following expression for the complex electro-mechanical admittance $\overline{Y}$

$$\overline{Y} = G + Bj = 4\omega\, j\frac{l^2}{h}\left[\overline{\varepsilon_{33}^{T}} - \frac{2d_{31}^2\overline{Y^E}}{(1-\nu)} + \frac{2d_{31}^2\overline{Y^E}}{(1-\nu)}\left(\frac{Z_{a,eff}}{Z_{s,eff}+Z_{a,eff}}\right)\overline{T}\right] \tag{13}$$

Here, a single complex term for $Z_{s,eff}$ (rather than four terms as in Zhou's model) accounts for the 2D mechanical interaction of the patch with the host structure. This makes the resulting equation simple enough to solve the inverse problem, i.e. to extract $Z_{s,eff}$ (Bhalla and Soh, 2004b), to be directly utilized for SHM/ NDE. No modelling is required for the host structure and the necessary data is directly obtainable from experimental measurements.

Annamdas and Soh (2007a) extended the 2D modeling to 3D, especially keeping in view thick PZT patches, by proposing a directional sum impedance model, taking into account the PZT patch's vibrations along all the three directions,. They defined the directional sum impedance as

$$Z_S = -(Z_{S1} + Z_{S2}) + Z_{S3} - 2Z_{12} + 2Z_{23} + 2Z_{31} \tag{14}$$

where the individual normal impedances (Z_{S1}, Z_{S2}, Z_{S3}) and the cross impedances (Z_{12}, Z_{23}, Z_{31}) are defined by Eqs.(15) and (16) respectively as

$$Z_{Si} = \frac{F_i}{u_i} \tag{15}$$

and $$Z_{ij} = -\frac{Z_{Si} Z_{Sj}}{Z_{Si} + Z_{Sj} - Z_{SK}} \quad (16)$$

The above definition resulted in a very set of complicated differential equations with no closed-form solution. As a simplification, the shear stress equation was ignored and the constants of integration proposed to be obtained through finite element analysis, thereby necessitating modelling of the structure concerned. The PZT patch also needs to be included in the model. Thus, the directional sum impedance approach could not be independently used with experimental data alone for solving the inverse problem.

In general, all the above models ignore the fact that the mechanical interaction between the PZT patch and the host structure occurs through a finitely thick layer of adhesive which, introduces the so-called 'shear lag effect' through its elastic deformation. This paper reviews the existing analytical approaches which model this aspect and proposes a new simplified model which is especially suitable for solving the inverse problem (of extracting Z_s), considering the presence of bond layer, in conjunction with the EMI technique. The main advantage over the previous models is that a closed-form analytical solution is derived which can be used directly with the measured G and B values, without necessitating any modelling for the host structure, bond layer or the PZT patch.

SHEAR LAG EFFECT

Fig. 4 illustrates the mechanism of physical deformation occurring in the PZT patch, the bond layer and the host structure for an adhesively-bonded PZT patch. Since force transmission occurs through the shearing of the bond layer, the displacement u (and hence strain) on the surface of the host structure is different from the displacement u_p (and hence strain) in the patch above.

This phenomenon is called the 'shear lag effect'. For the special case of a PZT patch bonded on a beam surface, and acting as a sensor, Sirohi and Chopra (2000) derived following expression for the strain ratio S_p/S_b (PZT strain to beam surface strain)

$$\frac{S_P}{S_b} = \left[1 - \frac{\cosh(\Gamma x)}{\cosh(\Gamma l)}\right] \tag{17}$$

where Γ is the shear lag parameter, given by

$$\Gamma = \sqrt{\frac{G_S}{Y^E h_S h_P} + \frac{3G_S w_P}{Y_b w_b h_b h_P}} \tag{18}$$

where h_p and h_S respectively denote the thicknesses of the patch and the bond layer, G_S the shear modulus of the bond layer, w_p and w_b respectively the widths of the patch and the beam, and Y^E and Y_b respectively the static Young's modulus of the patch and the beam.

Similarly, for a PZT patch acting as an actuator, the strains S_p and S_b were derived by Crawley and de Luis (1987) as

$$S_p = \frac{3\Lambda}{(3+\psi)} + \frac{\Lambda\psi\cosh\Gamma x}{(3+\psi)\cosh\Gamma l} \quad \text{and} \quad S_b = \frac{3\Lambda}{(3+\psi)} - \frac{3\Lambda\cosh\Gamma x}{(3+\psi)\cosh\Gamma l} \tag{19}$$

where $\Lambda = d_{31}E_3$ is the free piezoelectric strain, and $\psi = Y_b h_b / Y^E h_p$.

Integration of the shear lag effect into impedance modelling, especially for the EMI technique, was first attempted by Xu and Liu (2002). They included the bond layer in Liang's 1D impedance model by considering it as a single degree of freedom system connected in between the PZT patch and the impedance Z_s (of the host structure). The resultant equivalent impedance of the combination was determined as

$$Z_{eq} = \left[\frac{K_b}{K_b + K_S} \right] Z_S \tag{20}$$

where K_b represents the dynamic stiffness of the bond layer and K_S that of the structure. The effort, however, was incomplete, as no expression for K_b was derived. Ong et al. (2002) included the effect of the bond layer by considering strain variation as given by Eq. (17). This included the 'sensor effect', but invariably ignored the associated 'actuator effect'. In addition, the solution was restricted to beam structures only.

Bhalla and Soh (2004c) derived generalized formulations for electro-mechanical admittance across an adhesively bonded square PZT patch. By rigorously considering the deformation pattern shown in Fig. 4, following differential equation was derived for the 1D case

$$u'''' + \bar{p}u''' - qu'' = 0 \tag{21}$$

where u is the displacement on the surface of the host structure, below the PZT patch, and $\bar{p}$ and q the shear lag constants, given by

$$\bar{p} = -\frac{w_p \overline{G_s}}{Z_S h_S j\omega} \tag{22}$$

and

$$q = \frac{G_s}{Y^E h_S h_p} \tag{23}$$

Solving Eq. (21), the resultant mechanical impedance, called the 'equivalent impedance', was derived as

$$Z_{S,eq} = \frac{Z_S}{\left(1 + \frac{1}{\bar{p}} \frac{u_o'}{u_o}\right)} \tag{24}$$

where u_o is the displacement at the end of the PZT patch ($x = l$), to be determined from,

$$u = A_1 + A_2 x + Be^{\lambda_3 x} + Ce^{\lambda_4 x} \tag{25}$$

with

$$\lambda_3 = \frac{-\bar{p} + \sqrt{\bar{p}^2 + 4q}}{2} \text{ and } \lambda_4 = \frac{-\bar{p} - \sqrt{\bar{p}^2 + 4q}}{2} \tag{26}$$

The 1D approach was also extended to 2D effective impedance model and verified experimentally. This model was not only more rigorous but at the same time generic in nature. A parametric study revealed that to achieve best results, the adhesive layer should possess high shear modulus and minimum practicable thickness. A related experimental study has been reported by Qing et al. (2006). However, shortcoming of this model is visible for solving the inverse problem for NDE. In the damage quantification approach postulated by Bhalla and Soh (2004b), one needs to extract the mechanical impedance of the host structure ($Z_{s,} = x + yj$) from the measured admittance signature. In the presence of the adhesive layer, this would be $Z_{s,eq}$, from which it is computationally very difficult to obtain the true structural impedance Z_s, as clearly evident from Eqs. (21) to (26).

Annamdas and Soh (2007b) also extended their earlier formulations (2007a) for the case of an adhesive layer. However, no closed-form solution was derived. The adhesive layer needs to be included in the finite element model along with the host structure and the PZT patch. As with the earlier model of Annamdas and Soh (2007a), the approach is not able to solve the inverse problem with the measurement of *G* and *B* alone.

This difficulty of solving the inverse problem taking due consideration of the adhesive bond layer is very well alleviated by the simplified impedance model proposed in this paper. In the

next sections, the model is first derived first derived for 1D case and then extended to 2D situations.

NEW SIMPLIFIED 1 D IMPEDANCE MODEL

Fig.5 shows the physical aspects of the proposed simplified 1D impedance model. The PZT patch has length $2l$ with zero displacement at the mid point, which is the nodal point. Hence, only right half of the system is modelled here. The bond layer is assumed to be connected in between the PZT patch and the host structure such that it can transfer the force between the two through pure shear mechanism. Unlike the previous model of Bhalla and Soh (2004c), where shear strain varied along the patch, an average shear strain uniform along the length has been considered a s a simplification. Let u_p be the displacement at the tip of the PZT patch at any point of time. Due to the shearing of the bond layer, same displacement would not be transferred to the host structure. Let u be the displacement of the host structure at a point just underneath the tip of the PZT patch. Let h_p and h_S respectively denote the thickness of the patch and the bond layer. Shear strain in the bond layer is given by

$$\gamma = \frac{u_p - u}{h_s} \tag{27}$$

which can be rearranged as,

$$u = u_p - \left(\frac{\tau}{\overline{G_s}} \right) h_s \tag{28}$$

where τ denotes the interfacial shear stress and $\overline{G_S}$ the complex shear modulus of the bond layer. It should be noted that $\overline{G_S} = G_S(1 + \eta' j)$, where G_s is the static shear modulus and η' the associated mechanical loss factor of the bond layer. η' is strongly dependent on temperature and

can typically vary from 5% to 30% at room temperature, depending on the type of adhesive (Adams and Wake 1984). If F be the force transmitted to the host structure over the area A of one-half of the patch, Eq. (28) can be rewritten as

$$u = u_p - \left(\frac{F}{A\overline{G_S}} \right) h_s \tag{29}$$

Further, in terms of the structural impedance Z_s, the force transmitted to the host structure can be expressed as (Eq. 3)

$$F = -Z_S \dot{u} = -Z_S u j\omega \tag{30}$$

Substituting u from Eq. (29) and simplifying, we get

$$F = -Z_S j\omega \left[u_p - \frac{F h_S}{A\overline{G_S}} \right] \tag{31}$$

By rearranging the terms and with $A = wl$, Eq. (31) can be simplified as

$$F = -\frac{Z_S}{\left(1 - \frac{Z_S \omega h_s j}{wl\overline{G_s}} \right)} j\omega u_p \tag{32}$$

This can be expressed in a format similar to Eq. (30) as

$$F = -Z_{S,eq} j\omega u_p \tag{33}$$

where

$$Z_{S,eq} = \frac{Z_S}{\left(1 - \frac{Z_S \omega h_s j}{wl\overline{G_s}} \right)} \tag{34}$$

is the 'equivalent impedance', apparent at the ends of the PZT patch, taking into consideration the shear lag phenomenon associated with the bond layer. Replacing $Z_{s,}$ by $Z_{s,eq}$ in Eq. (7), the modified expression for admittance across the PZT patch results as

$$\overline{Y} = G + Bj = 2\omega j \frac{wl}{h}\left[(\overline{\varepsilon_{33}^{T}} - d_{31}^{2}\overline{Y^{E}}) + \left(\frac{Z_a}{Z_{s,eq} + Z_a} \right) d_{31}^{2}\overline{Y^{E}} \left(\frac{\tan \kappa l}{\kappa l} \right) \right] \tag{35}$$

EXTENSION TO 2 D EFFECTIVE IMPEDANCE BASED IMPEDANCE MODEL

This section extends the 1D shear lag based impedance formulations derived above to 2D effective impedance-based electromechanical model proposed by Bhalla and Soh (2004a). The PZT patch is assumed to be square in shape with a half-length equal to *l*. The strain distribution and the associated shear lag are determined along each principal direction independently, invariably introducing discontinuity at the corners, which is ignored. By applying Eq. (29) along each principal direction for the configuration of Fig. 3b (for a quarter of the patch),

$$u_1 = u_{p1} - \left(\frac{F_1}{l^2 \overline{G_s}} \right) h_s \tag{36}$$

and

$$u_2 = u_{p2} - \left(\frac{F_2}{l^2 \overline{G_s}} \right) h_s \tag{37}$$

where F_1 and F_2 are the forces along each direction as shown in Fig. 3(b). Adding Eqs. (36) and (37) and dividing by 2, we get

$$\frac{u_1 + u_2}{2} = \frac{u_{p1} + u_{p2}}{2} - \left(\frac{F_1 + F_2}{2l^2 \overline{G_s}} \right) h_s \tag{38}$$

From the definition of effective displacement (Bhalla and Soh, 2004a)

$$u_{eff} = \frac{\delta A}{p_o} = \frac{u_1 l + u_2 l + u_1 u_2}{2l} \approx \frac{u_1 + u_2}{2} \tag{39}$$

Further, from Eq. (11),

$$F_{eff} = F_1 + F_2 \tag{40}$$

Thus, using Eqs. (39) and (40), Eq. (38) can be reduced to

$$u_{eff} = u_{p,eff} - \left(\frac{F_{eff}}{2l^2 \overline{G_s}} \right) h_s \tag{41}$$

From the definition of effective impedance,

$$F_{eff} = -Z_{eff} u_{eff} j\omega \tag{42}$$

Substituting Eq. (41) into (42) and solving, as for the 1D case, an expression for the equivalent effective impedance can be derived as

$$Z_{s,eff,eq} = \frac{Z_{s,eff}}{\left(1 - \frac{Z_{s,eff} \omega h_s j}{2l^2 \overline{G_s}} \right)} \tag{43}$$

With the above result, Eq. (13) can be modified, by replacing Z_{eff} by $Z_{s,eff,eq}$ as

$$\overline{Y} = G + Bj = 4\omega \, j \frac{l^2}{h} \left[\overline{\varepsilon_{33}^T} - \frac{2d_{31}^2 \overline{Y^E}}{(1-\nu)} + \frac{2d_{31}^2 \overline{Y^E}}{(1-\nu)} \left(\frac{Z_{a,eff}}{Z_{s,eff,eq} + Z_{a,eff}} \right) \overline{T} \right] \tag{44}$$

In order to verify the proposed new model, an aluminium block, 48x48x10mm in size, was considered as the host structure. A PZT patch, 10x10x0.3mm in size, was assumed to be surface-bonded on this structure. Fig. 6 shows the 3D finite element model of a quarter of the host structure. The effective drive point impedance of the host structure was computed by carrying out 3D dynamic harmonic analysis, as outlined by Bhalla and Soh (2004a). The PZT patch or the bond layer need not be meshed since their stiffness, mass and damping are separately considered in the formulations. The physical properties of Al 6061-T6 were considered as: Young's modulus = 68.95GPa, density = 2715 kg/m^3 and Poisson's ratio = 0.33. Rayleigh damping was considered with $\alpha = 0$ and $\beta = 3 \times 10^{-9}$. Wavelength analysis and convergence test on this model has already been reported by Bhalla and Soh (2004a). A uniformly distributed planar harmonic force was applied along the boundary of the PZT patch and the displacement response was

obtained by full dynamic harmonic analysis to determine the effective drive point impedance of the structure as

$$Z_{s,eff} = \frac{F_{eff}}{j\omega u_{eff}} \tag{45}$$

Final values for G and B were determined in the frequency range 0-250kHz using Eq. (44). A 0.150mm thick epoxy layer was considered with shear modulus of G_s = 1 GPa and a mechanical loss factor of η' = 10%. The parameters of the PZT patch considered are listed in Table 1.

Fig. 7 shows a comparison of the variation of conductance with frequency obtained using the present model and also the previous model of Bhalla and Soh (2004c). Curves obtained by both models are plotted alongside the curves for the case of perfect bonding for comparison. The proposed simplified model predicts the conductance in consistency with the results of Bhalla and Soh (2004c).Both the models predict that the peaks tend to diminish down due to the presence of the bond layer. Similarly, Fig. 8 shows a comparison of the variation of susceptance for three cases- no bond layer, Bhalla and Soh (2004c) model and the proposed simplified model. It is observed that like the previous model, the new simplified model leads to the observation that peaks lose their sharpness and the average slope of the susceptance curve tends to reduce owing to the shear lag effect. However, the susceptance curve resulting from the present model lies intermediate of the two cases i.e perfect bond and the model of Bhalla and Soh (2004c).

The influence of important parameters on the conductance and susceptance signatures was studied using the new simplified model and the observations compared with the previous model. Fig. 9 shows the influence of the bond layer's shear modulus on conductance signatures. Three values of G_s = 1.0 GPa, 0.5 GPa and 0.05 GPa were considered for a bond layer thickness of

0.15mm. It is observed that as G_s decreases, peaks of the conductance plot subside down. Worst effect is observed for the case G = 0.05GPa, for which the PZT patch behaves independent of the host structure. Fig. 10 similarly shows the influence of G_s on susceptance, for which case the average slope of the curve decreases in addition to the peaks subsiding down. For G_S = 0.05 GPa, again the patch seems to behave independent of the structure. Similar observations were reported by Bhalla and Soh (2004c). Fig. 11 shows the influence of bond layer thickness on conductance, by considering two values h_s = 0.1mm (h_s/h_p = 0.33) and 0.150mm (h_s/h_p = 0.5). It is observed that with increase of the bond layer's thickness, the peaks subside down (notice peaks marked P_1 and P_2 in Fig. 11). Fig. 12 shows the corresponding curves for susceptance, for which it is observed that the peaks as well as the average slope of the curve subside down. The effect of increase in bond layer's thickness is thus similar to that of reduction of G_S. Fig. 13 shows the influence of bond layer's damping, for three values of η' =5%, 10% and 15% for a constant G_s = 1GPa and bond layer thickness of 0.150mm. It is observed that this factor has small influence on conductance, where the average slope of the curve appears to slightly reduce but virtually no effect on susceptance signatures, an observation matching with Bhalla and Soh (2004c).

PRACTICAL RELEVANCE OF NEW MODEL

The results presented in the previous section show that in spite of its simplicity, the new model produces results, comparable to the previous model of Bhalla and Soh (2004c) that was analytically far more complicated . The main strength of the new shear lag model is the simplicity of application for solving the inverse problem. As pointed out above, it is computationally very difficult to obtain the true structural impedance $Z_{s,eff}$ from $Z_{s,eff,eq}$, using the

previous model for adhesively bonded PZT patches. On the other hand, using the new simplified model, the true structural impedance can be directly determined, from Eq. (43) as,

$$Z_{s,eff} = \frac{2l^2 \overline{G_s} Z_{s,eff,eq}}{2l^2 \overline{G_s} + Z_{s,eff,eq} \omega h_s j} \tag{46}$$

. $Z_{s,eff,eq}$ can be obtained from the measured G and B directly using the equations derived by Bhalla and Soh (2004c) for use in Eq. (46) above. No modelling is required for the host structure or the bond layer The finite element modelling done in the previous section was solely for model verification purpose only and not required in the actual applications where G and B will be available through measurement. The true structural mechanical impedance can be conveniently used for SHM of structural and aerospace components using the method proposed by Bhalla and Soh (2004 b).

Fig. 14 compares the extracted structural impedance for an aluminium block 48x48x10mm, with and without considering the bond layer. $Z_{s,eff,eq}$ is derived from the experimentally obtained admittance signatures (Bhalla and Soh, 2004a, b) followed by $Z_{s,eff,}$ using Eq. (46). It is observed that the ignoring the bond layer tends to overestimate the structural true impedance. This is because the bond layer offers additional impedance on account of its own stiffness, damping and inertia. Solving the inverse problem assuming perfect bond results into impedance "apparent " at the patch ends, i.e with bond layer included . On the other hand, using the proposed formulations eliminates the effect of the bond layer and hence the impedance gets reduced. To determine the true impedance using the previous model would have demanded solving 4^{th} order differential equation, which is circumvented by the new simplified model.

CONCLUSIONS

This paper has presented the development of a new simplified impedance model incorporating the shear lag effect into electro-mechanical admittance formulations. The model is first developed for 1D case and then extended to 2D case. The results of the model have been compared with those of the Bhalla and Soh's shear lag impedance model (2004c). Further, a detailed parametric study on conductance and susceptance signatures has been carried out. Although far simplified, the proposed model is found to predict the conductance and the susceptance signatures in close proximity with those predicted by the model of Bhalla and Soh (2004c). The advantages of the new model are quite apparent. This model simplifies the complex shear lag phenomenon associated with the force transmission between the PZT patch and the host structure bonded to each other by the adhesive bond layer. It enables computing the true mechanical impedance of the structure from the measured experimental data alone, thus circumventing the necessity of preparing a model of the host structure or the bond layer.

NOTATIONS

C_1 , C_2 (*or* C) = Peak correction factors for PZT patch

d_{im} = Piezoelectric strain coefficient (or constant)

d_{31} = Piezoelectric strain coefficient corresponding to x-z (or 1-3) axis

D_i = Component of electric displacement vector

E_j = Component of electric field vector

F_{eff} = Effecive force

f = Boundary traction per unit length

$\overline{G_s}$ = Complex shear modulus of elasticity of bond layer

h = Thickness

h_b = Thickness (depth) of beam

h_p = Thickness of PZT patch

h_S = Thickness of bond layer

$\overline{K_b}$ = Dynamic stiffness of bond layer

$\overline{K_S}$ = Dynamic stiffness of structure

l = Half-length

$\hat{n}$ = Unit vector normal to the boundary

p_o = Perimeter of PZT patch in the undeformed condition

$\overline{p}$, q = Shear lag parameters for 1D model of Bhalla and Soh (2004c)

$\overline{p_{eff}}$, q_{eff} = Shear lag parameters for 2D model of Bhalla and Soh (2004c)

S_k	=	Component of mechanical strain tensor
S_1	=	Strain along axis 1.
S_b	=	Surface strain on beam
S_P	=	Axial strain in PZT patch
$\overline{T}$	=	Complex tangent ratio
T_m	=	Component of mechanical stress tensor
$\overline{s_{km}^E}$	=	Component of elastic compliance tensor at constant electric field
u_1, u_2	=	Edge displacements of host structure along principal directions
u_{p1}, u_{p2}	=	Edge displacements of PZT patch along principal directions
$u_{p,eff}$	=	Effective displacement of PZT patch
u_{eff}	=	Effective displacement of host structure
w	=	Width
w_b	=	Width of beam
w_p	=	Width of PZT patch
$\overline{Y}$	=	Complex electrical admittance
$\overline{Y^E}$	=	Complex Young's modulus of PZT patch at constant electric field
Y_b	=	Static Young's modulus of elasticity of the beam
Z_s	=	Structural mechanical impedance (1D case)
Z_a	=	Mechanical impedance of the PZT patch (1D case)
$Z_{s,eq}$	=	Equivalent structural mechanical impedance including shear lag effect (1D case)

$Z_{s,eff}$	=	Effecive mechanical impedance of structure (2D case)
$Z_{a,eff}$	=	Effecive mechanical impedance of patch (2D case)
$Z_{s,eff,eq}$	=	Equivalent effective mechanical impedance of structure including shear lag effect (2D case)
$\overline{\varepsilon_{ij}^{T}}$	=	Component of complex electric permittivity tensor of PZT material at constant stress
$\overline{\varepsilon_{33}^{T}}$	=	Complex electric permittivity of the PZT material at constant stress along axis 3
η	=	Mechanical loss factor of PZT patch
η'	=	Mechanical loss factor of bond layer
δ	=	Dielectric loss factor of PZT patch
ψ	=	$(Y_b h_b / Y^E h_p)$, product of modulus and thickness ratios of beam and PZT patch
Λ	=	Free piezoelectric strain (= $d_{31} E_3$)
ω	=	Angular frequency
τ	=	Interfacial shear stress
Γ	=	Shear lag parameter
γ	=	Shear strain in bond layer
κ	=	Wave number
δA	=	Change in the surface area of PZT patch

REFERENCES

Adams, R. D. and Wake, W. C. (1984). *Structural adhesive joints in engineering*, Elsevier Applied Science Publishers, London.

Annamdas, V. G. M. and Soh, C. K. (2007a). "Three-dimensional electromechanical impedance model: formulation of directional sum impedance." *J. Aerospace Engineering*, ASCE, 20(1), 53-62.

Annamdas, V. G. M. and Soh, C. K. (2007b). "An electromechanical impedance model of a piezoceramic transducer-structure in the presence of thick adhesive bonding." *Smart Materials and Structures*, 16(3), 673-686.

ANSYS Inc. (2000). *ANSYS reference manual*, release 5.6, Canonsburg, PA.

Bhalla, S. and Soh, C. K. (2003). "Structural impedance based damage diagnosis by piezo-transducers." *Earthquake Engineering and Structural Dynamics*, 32(12), 1897-1916.

Bhalla, S. and Soh, C. K. (2004a). "Structural health monitoring by piezo-impedance transducers I: modeling." *J. Aerospace Engineering*, ASCE, 17(4), 154-165.

Bhalla, S. and Soh, C. K. (2004b). "Structural health monitoring by piezo-impedance transducers II: Applications." *J. Aerospace Engineering*, ASCE, 17(4), 166-175.

Bhalla, S. and Soh, C. K. (2004c). "Impedance based modeling for adhesively bonded piezo-transducers." *J. Intelligent Material Systems and Structures*, 15(12), 955-972.

Crawley, E. F., de Luis, J. (1987). "Use of piezoelectric actuators as elements of intelligent structures." *AIAA Journal*, 25(10), 1373-1385.

Giurgiutiu, V. and Zagrai, A. N. (2002). "Embedded self-sensing piezoelectric active sensors for on-line structural identification." *Journal of Vibration and Acoustics*, ASME, (124), 116-125.

IEEE (1987). Std. 176, IEEE *Standard on piezoelectricity,* IEEE.

Liang, C., Sun, F. P. and Rogers, C. A. (1994). "Coupled electro-mechanical analysis of adaptive material systems- determination of the actuator power consumption and system energy transfer", *J. Intelligent Material Systems and Structures*, 5, 12-20.

Ong, C.W., Yang, Y., Wong, Y.T., Bhalla, S., Lu, Y. and Soh, C.K. (2002). "The effects of adhesive on the electro-mechanical response of a piezoceramic transducer coupled smart system." *Proc. ISSS-SPIE International Conference on Smart Materials, Structures and Systems*, 12-14 December, Bangalore, 191-197.

Park, G., Cudney, H. H. and Inman, D. J. (2000). "Impedance-based health monitoring of civil structural components." *Journal of Infrastructure Systems*, ASCE, 6(4), 153-160.

Park, S. Yun, C.- B., Roh, Y. and Lee, J.- J. (2006). "PZT-based active damage detection techniques for steel bridge components." *Smart Materials and Structures*, 15(4), 957-966.

Qing, X. P., Chan, H.- L., Beard, S. J., Ooi, T. K., Marotta, S. A. (2006). "Effect of adhesive on performance of piezoelectric elements used to monitor structural health." *International Journal of Adhesion and Adhesives*, 26(8), 622-628.

Sirohi, J. and Chopra, I. (2000). "Fundamental understanding of piezoelectric strain sensors." *J. Intelligent Material Systems and Structures*, 11(4), 246-257.

Soh, C. K., Tseng, K. K.-H., Bhalla, S. and Gupta, A. (2000). "Performance of smart piezoceramic patches in health monitoring of a RC bridge." *Smart Materials and Structures*, 9(4), 533-542.

Sun, F. P., Chaudhry, Z., Rogers, C. A., Majmundar, M. and Liang, C. (1995). "Automated real-time structure health monitoring via signature pattern recognition", , *Proc. SPIE*

Conference on Smart Structures and Materials, San Diego, California, Feb.27-Mar1, 2443, 236-247.

Xu, Y. G. and Liu, G. R. (2002). "A modified electro-mechanical impedance model of piezoelectric actuator-sensors for debonding detection of composite patches", *J. Intelligent Material Systems and Structures*, 13(6), 389-396.

Zhou, S. W., Liang, C. and Rogers C. A. (1996). "An impedance-based system modeling approach for induced strain actuator-driven structures", *Journal of Vibrations and Acoustics*, ASME, 118(3), 323-331.

LIST OF FIGURES AND TABLES

Fig. 1 (a) Liang's 1D impedance model.
(b) A PZT patch surface-bonded to a structure.
(c) Impedance model for the system shown in (b).

Fig. 2 2D impedance model of Zhou et al. (1996).

Fig. 3 Effective impedance model of Bhalla and Soh (2004a).
(a) PZT bonded to host structure. (b) Interaction forces at boundary.

Fig. 4 Deformation in bond layer and PZT patch.

Fig. 5 Proposed simplified 1D impedance model (showing right symmetrical half of PZT patch-structure system.

Fig. 6 3D finite element model of one-quarter of test structure.

Fig. 7 Comparison of conductance signature.
(a) Bhalla and Soh's model. (b) New simplified model.

Fig. 8 Comparison of susceptance signature from new model with Bhalla and Soh (2004c) model.

Fig. 9 Influence of shear modulus of elasticity on conductance signatures.
(a) Perfect bond (b) G = 1GPa (c) G = 0.5GPa (d) G = 0.05GPa

Fig. 10 Influence of shear modulus of elasticity on susceptance signatures.

Fig. 11 Influence of bond layer thickness on conductance signatures.
(a) Perfect bond (b) h_s = 0.1mm (c) h_s = 0.15mm

Fig. 12 Influence of bond layer thickness on susceptance signatures.

Fig. 13 Influence of r bond layer damping.
(a) Conductance vs frequency. (b) Susceptance vs frequency.

Fig. 14 Considering influence of bond layer to extract structural mechanical impedance.

Table 1 Key parameters of PZT patch

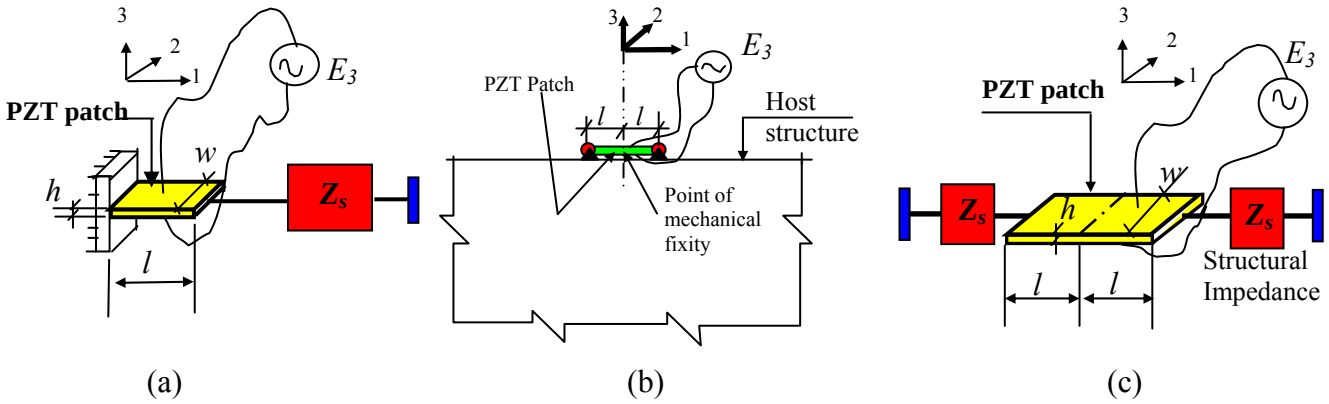

Fig. 1 (a) Liang's 1D impedance model (Liang et al. 1994).
(b) A PZT patch surface-bonded to a structure.
(c) Impedance model for the system shown in (b).

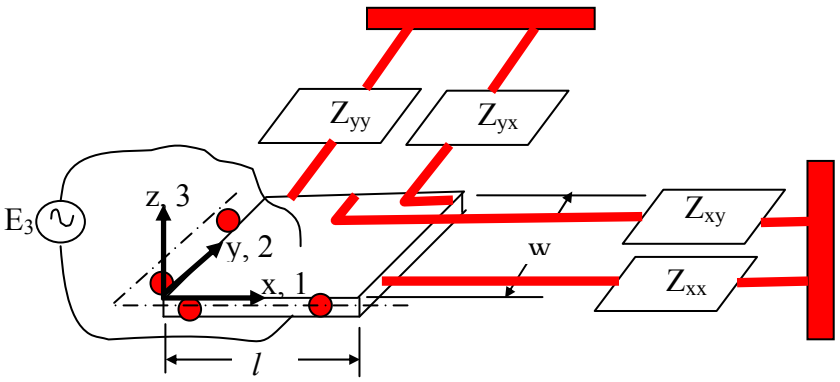

Fig. 2 2D impedance model of Zhou et al. (1996).

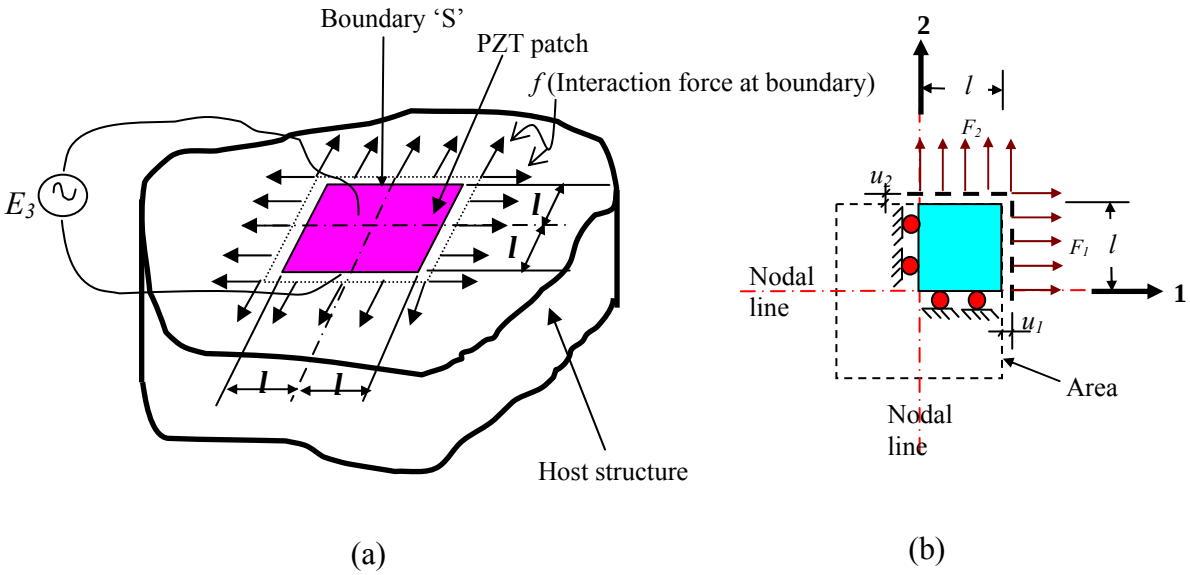

Fig. 3 Effective impedance model of Bhalla and Soh (2004a).

(a) PZT bonded to host structure. (b) Interaction forces at boundary.

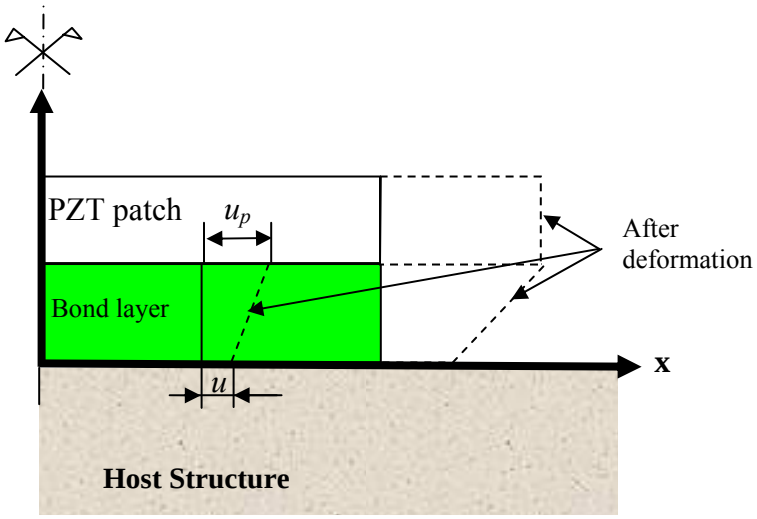

Fig. 4 Deformation in bond layer and PZT patch.

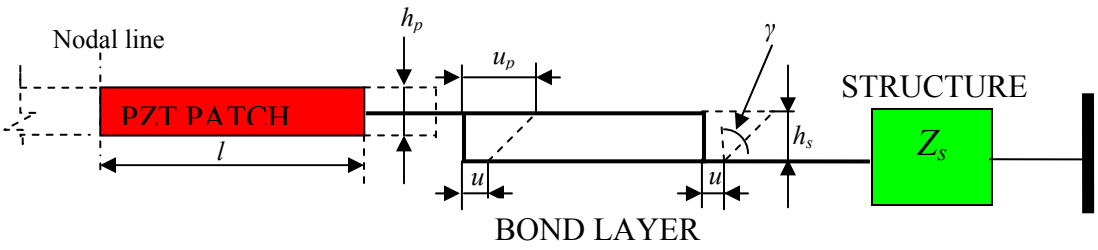

Fig. 5 Proposed simplified 1D impedance model (showing right symmetrical half of PZT patch- structure system.

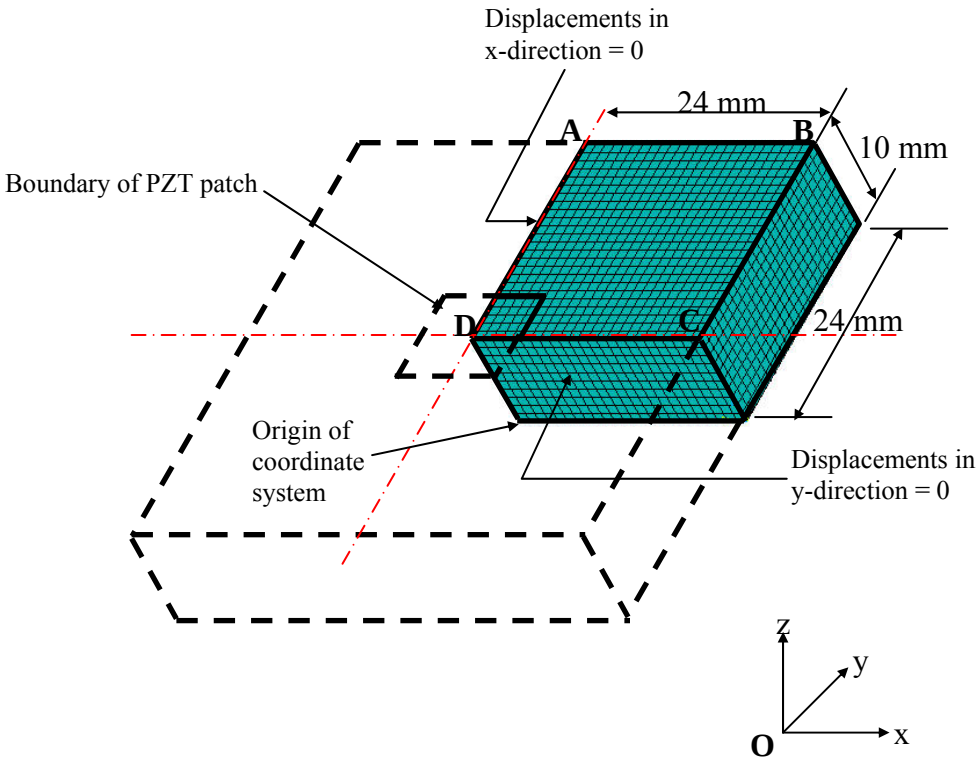

Fig. 6 3D finite element model of one-quarter of structure.

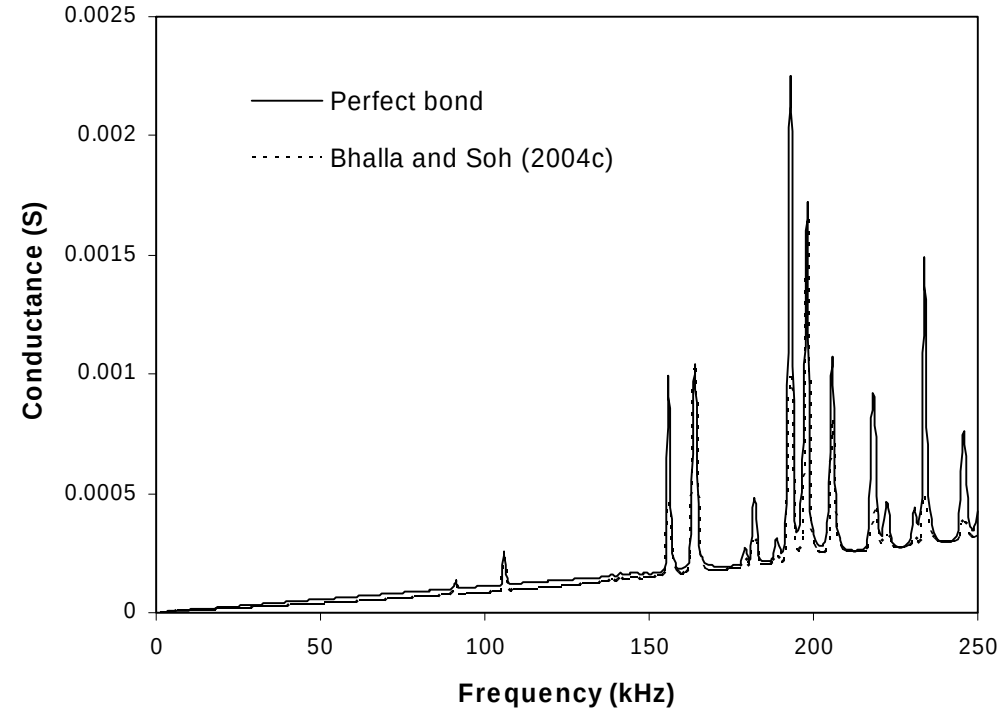

(a)

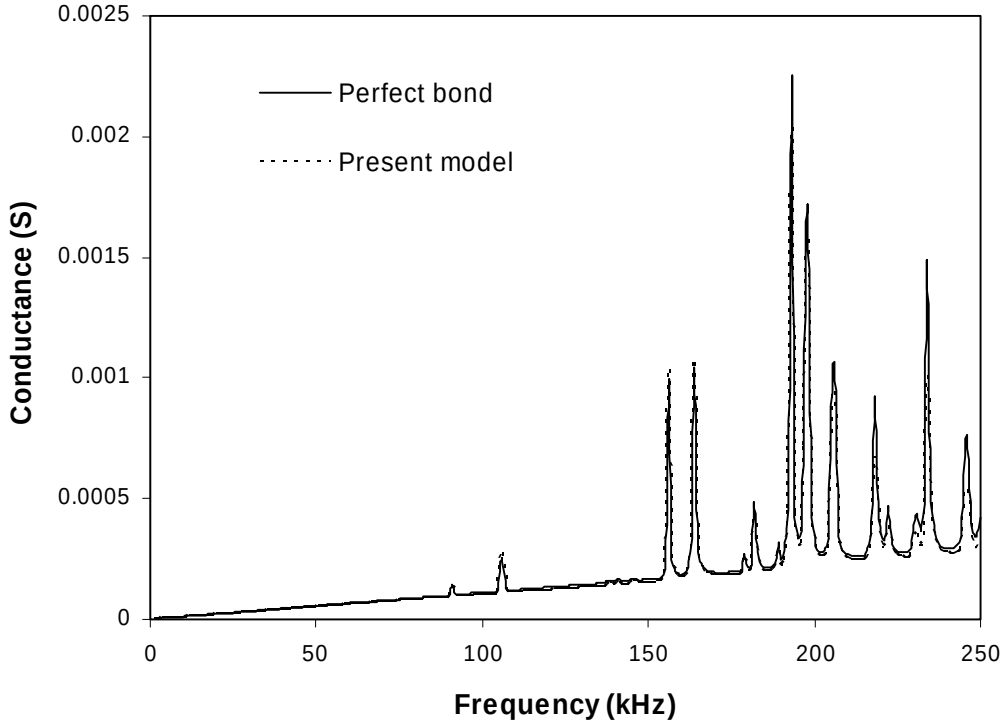

(b)

Fig. 7 Comparison of conductance signature.

(a) Bhalla and Soh's model. (b) New simplified model.

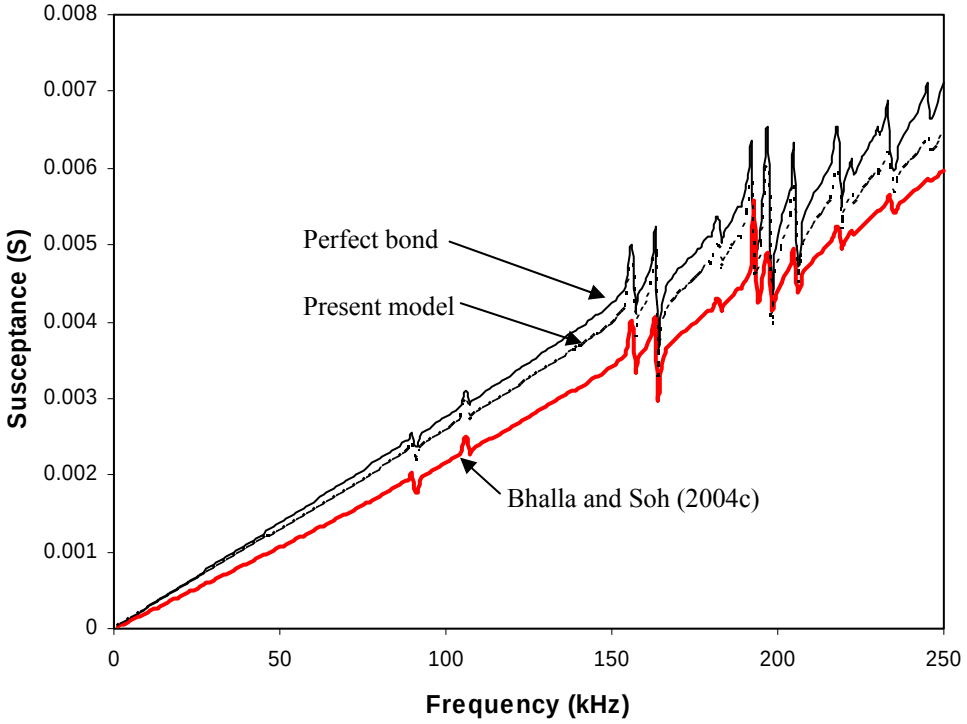

Fig. 8 Comparison of susceptance signature from new model with Bhalla and Soh (2004c) model.

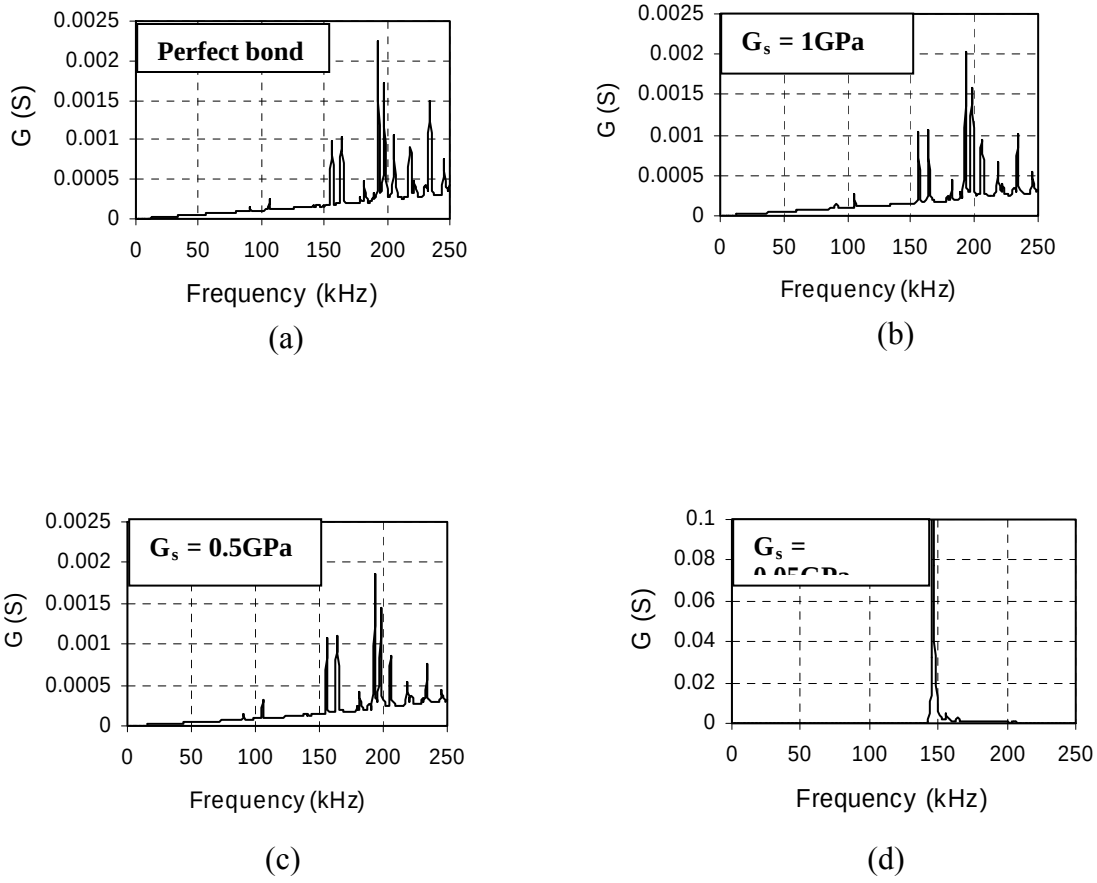

Fig. 9 Influence of shear modulus of elasticity on conductance signatures.

(a) Perfect bond (b) G_S = 1GPa (c) G_S = 0.5GPa (d) G_S = 0.05GPa

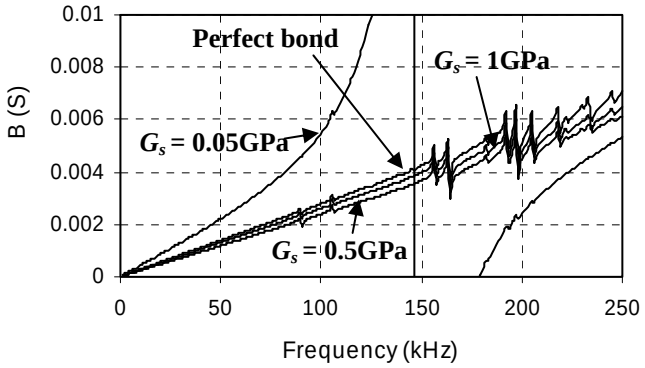

Fig. 10 Influence of shear modulus of elasticity on susceptance signatures.

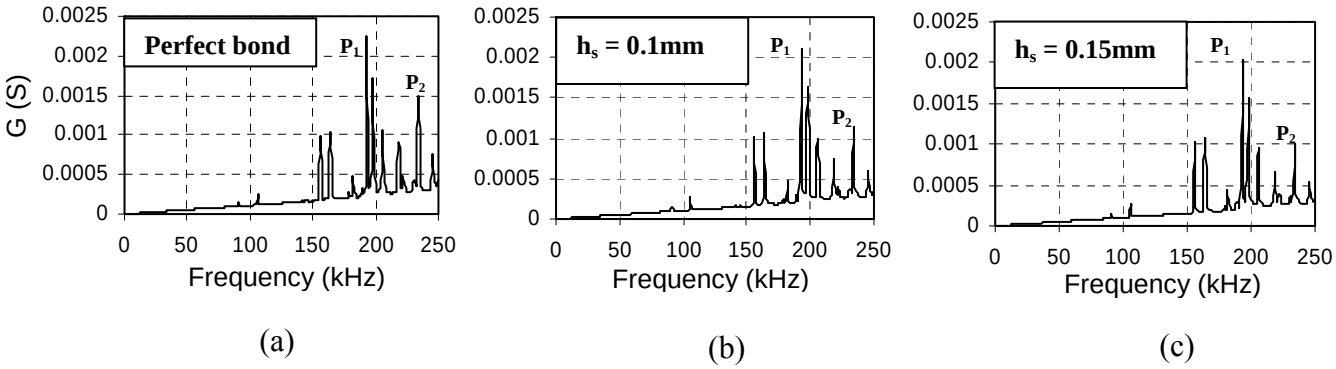

Fig. 11 Influence of bond layer thickness on conductance signatures.

(a) Perfect bond (b) h_s = 0.1mm (h_s/h_p =0.33) (c) h_s = 0.15mm (h_s/h_p = 0.5)

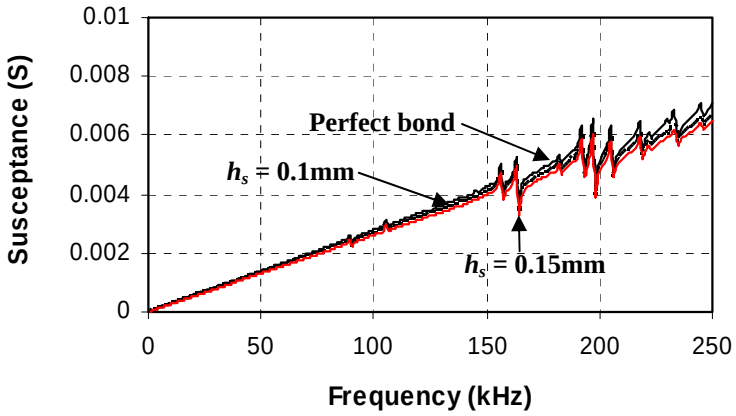

Fig. 12 Influence of bond layer thickness on susceptance signatures.

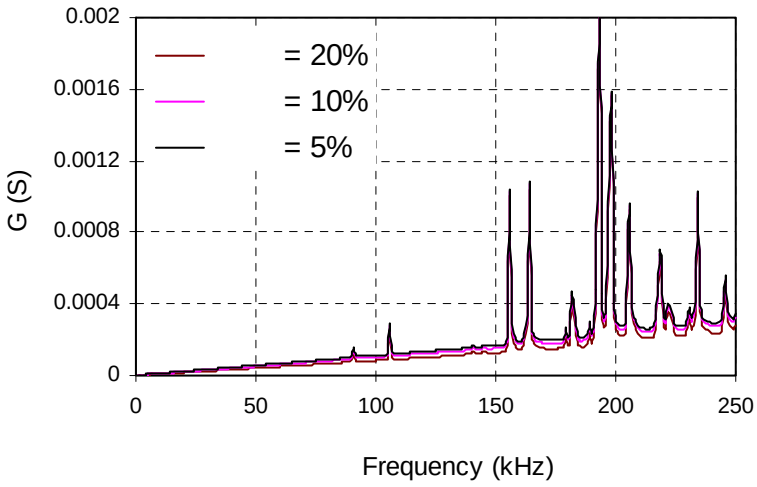

(a)

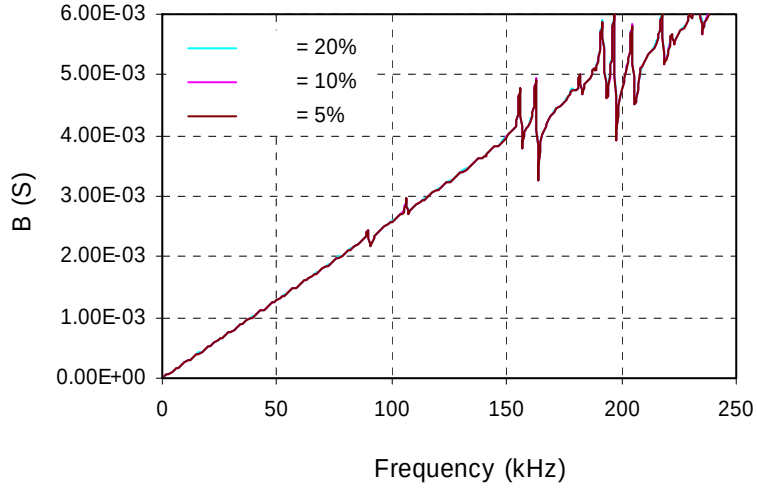

(b)

Fig. 13 Influence of r bond layer damping.

(a) Conductance vs frequency. (b) Susceptance vs frequency.

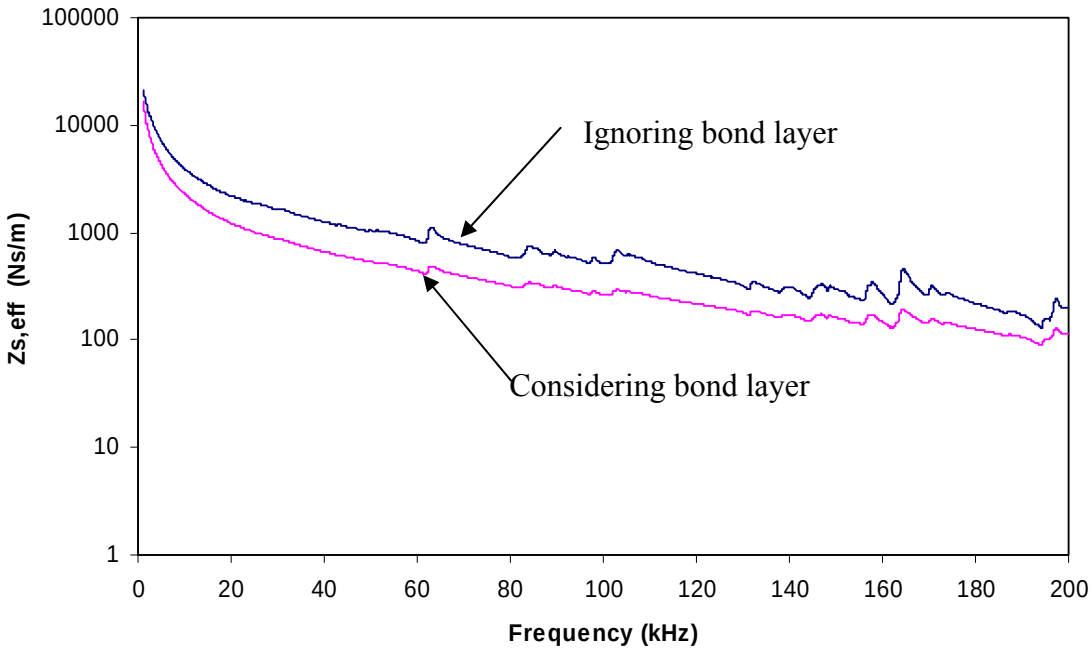

Fig. 14 Considering influence of bond layer to extract structural mechanical impedance.

B

Table 1 Parameters of PZT patches considered.

Physical Parameter	Value
Electric Permittivity, ε_{33}^{T} (Farad/m)	1.7785×10^{-8}
Peak correction factor, C_f	0.898
$K = \frac{2d_{31}^2 Y^E}{(1-\upsilon)}$ (N/V^2)	5.35×10^{-9}
Mechanical loss factor, η	0.0325
Dielectric loss factor, δ	0.0224